Common general anesthetic propofol impairs kinesin processivity

Brandon M. Bensel[a,b,1], Stephanie Guzik-Lendrum[a,b,1], Erin M. Masucci[a,b], Kellie A. Woll[c], Roderic G. Eckenhoff[c], and Susan P. Gilbert[a,b,2]

[a]Department of Biological Sciences, Rensselaer Polytechnic Institute, Troy, NY 12180; [b]Center for Biotechnology and Interdisciplinary Studies, Rensselaer Polytechnic Institute, Troy, NY 12180; and [c]Department of Anesthesiology and Critical Care, University of Pennsylvania Perelman School of Medicine, Philadelphia, PA 19104

Edited by Michael L. Klein, Temple University, Philadelphia, PA, and approved April 12, 2017 (received for review January 27, 2017)

Propofol is the most widely used i.v. general anesthetic to induce and maintain anesthesia. It is now recognized that this small molecule influences ligand-gated channels, including the $GABA_A$ receptor and others. Specific propofol binding sites have been mapped using photoaffinity ligands and mutagenesis; however, their precise target interaction profiles fail to provide complete mechanistic underpinnings for the anesthetic state. These results suggest that propofol and other common anesthetics, such as etomidate and ketamine, may target additional protein networks of the CNS to contribute to the desired and undesired anesthesia end points. Some evidence for anesthetic interactions with the cytoskeleton exists, but the molecular motors have received no attention as anesthetic targets. We have recently discovered that propofol inhibits conventional kinesin-1 KIF5B and kinesin-2 KIF3AB and KIF3AC, causing a significant reduction in the distances that these processive kinesins can travel. These microtubule-based motors are highly expressed in the CNS and the major anterograde transporters of cargos, such as mitochondria, synaptic vesicle precursors, neurotransmitter receptors, cell signaling and adhesion molecules, and ciliary intraflagellar transport particles. The single-molecule results presented show that the kinesin processive stepping distance decreases 40–60% with EC_{50} values <100 nM propofol without an effect on velocity. The lack of a velocity effect suggests that propofol is not binding at the ATP site or allosteric sites that modulate microtubule-activated ATP turnover. Rather, we propose that a transient propofol allosteric site forms when the motor head binds to the microtubule during stepping.

anesthesia | allosteric inhibitor | microtubule | etomidate | ketamine

Propofol (2,6-diisopropylphenol) is the most widely used i.v. general anesthetic to induce and maintain anesthesia (1, 2). The consensus to date has been that general anesthetics, like propofol, are small hydrophobic molecules that bind to ligand- or voltage-gated channels, and it is the change in their activities that elicits the end points of anesthesia, including behavioral immobility, amnesia, and loss of consciousness. Propofol influences ligand-gated channels, including the $GABA_A$ receptor as well as other ligand-gated channels and receptors (3–8). Moreover, specific propofol binding sites have been mapped using photoaffinity ligands and mutagenesis. However, their precise target interaction profiles have not yet satisfied the criteria of being both necessary and sufficient to produce the complete anesthetic state (4–9). This body of work suggests that propofol and other common anesthetics, such as etomidate and ketamine (10–14), may target additional protein networks of the CNS, including potential interactions with the cytoskeleton to contribute to the desired and undesired anesthesia end points. Some evidence for anesthetic interactions with the cytoskeleton exist (15–18). For example, different classes of general anesthetics bind specifically to tubulin and alter its stability (17, 18), and entire theories of anesthetic action have been constructed around microtubule (MT) properties (19). However, the molecular motors that travel along MTs have received no attention as anesthetic targets. We have recently discovered that propofol inhibits three processive kinesins (kinesin-1 KIF5B, kinesin-2 KIF3AB, and kinesin-2 KIF3AC) using single-molecule motility assays. These in vitro assays are powerful in that they can assess the ability of a single dimeric motor to step along a MT. Propofol caused a significant reduction in the potential distance that these kinesins can travel. These MT-based motors are highly expressed in the CNS and the major anterograde transporters of cargos, such as mitochondria, synaptic vesicle precursors, neurotransmitter receptors, cell signaling and cell adhesion molecules, mRNA particles, and ciliary intraflagellar transport particles (20–25). The results presented provide a compelling inhibition profile to hypothesize that kinesins may also be targets of general anesthetics, such as propofol, etomidate, and/or ketamine, and thereby, contribute to the state of general anesthesia.

Results

Propofol Decreases the Persistence of MT Gliding but Does Not Alter the Velocity of Movement. To test the hypothesis that propofol can affect kinesin motility, a MT gliding assay was used in conjunction with total internal reflection fluorescence (TIRF) microscopy (26, 27). The advantage of this assay is that it evaluates the ability of the motor population to propel and sustain MT gliding across a lawn of kinesin motors. The first experiment tested the well-characterized homodimeric kinesin-1 K560 (27–29). K560 was bacterially expressed from human kinesin-1 *KIF5B*, encoding

Significance

Kinesins are major transporters of cargos toward the cell periphery. They are highly expressed in the CNS, and their dysfunction leads to a wide range of human pathologies, including neurodevelopmental and neurodegenerative diseases, ciliopathies, epilepsy, and birth defects. We have discovered that the widely used general anesthetic propofol shortens the distance that kinesins travel, but their velocity remains unchanged. These results suggest that propofol is not binding at the ATP site or allosteric sites that affect ATP turnover, leading to the conclusion that the allosteric sites form on microtubule association. We postulate that general anesthetics bind specifically to transport kinesins and/or the kinesin–β-tubulin interface, and diminish their ability to transport critical cargos, thereby contributing to the pleiotropic state of anesthesia.

Author contributions: S.G.-L., R.G.E., and S.P.G. designed research; B.M.B., S.G.-L., E.M.M., and K.A.W. performed research; R.G.E. and S.P.G. contributed new reagents/analytic tools; B.M.B., S.G.-L., E.M.M., K.A.W., and S.P.G. analyzed data; and B.M.B., S.G.-L., K.A.W., R.G.E., and S.P.G. wrote the paper.

The authors declare no conflict of interest.

This article is a PNAS Direct Submission.

[1]B.M.B. and S.G.-L. contributed equally to this work.

[2]To whom correspondence should be addressed. Email: sgilbert@rpi.edu.

This article contains supporting information online at www.pnas.org/lookup/suppl/doi:10.1073/pnas.1701482114/-/DCSupplemental.

the first 560 amino acid residues. A 10-μL perfusion chamber was constructed, and antibodies to the C-terminal His tag of K560 were applied followed by perfusion of MT–K560 complexes. This approach ensures tight binding of the C terminus of K560 to the coverslip. Subsequently, K560 motility was initiated by 1 mM MgATP. The results in Fig. 1 show that, in the presence of 5 μM propofol, the MTs initially glided across the K560 coverslip as in the DMSO control, but the number of K560-associated MTs decreased dramatically as a function of time as MTs detached from the coverslip and were no longer illuminated in the TIRF field (Movies S1 and S2). Moreover, MT stalling on the coverslip was rarely observed in the presence of propofol. After 5 min, ∼80% of MTs glide persistently, but by 20 min, the population remaining on the kinesin-coated surface dropped to 59.3%. These results were in stark contrast to the DMSO control, where ∼95% of the MT population was observed to glide continuously across the K560 coverslip (Fig. 1*G*).

The MT gliding assay was repeated for kinesin-2 KIF3AC (Fig. 1 *B*, *E*, and *H*) and KIF3AB (Fig. 1 *C*, *F*, and *I*). These kinesins are distinctive in that they exist physiologically as heterodimers formed from three different gene products: *KIF3A*, *KIF3B*, and *KIF3C* (21–24, 30). The KIF3AC and KIF3AB heterodimers, characterized previously, were engineered to include the N-terminal native motor domain sequence, neck linker, and native helix α7 followed by a dimerization motif to stabilize the native coiled coil (27, 31). The results in Fig. 1 also show that KIF3AC and KIF3AB were similarly affected by 5 μM propofol, such that the persistence of MT gliding decreased to 52.3% of the MT population for KIF3AC and 51.9% of the MT population for KIF3AB. Although propofol altered the persistence of MT gliding by K560, KIF3AC, and KIF3AB, it surprisingly did not alter MT gliding velocity (Fig. 1 *A*–*F*). These results indicate that propofol did not affect ATP turnover but rather, altered the processivity of individual kinesin motors. To test this hypothesis directly, single-molecule quantum dot (Qdot) motility assays were pursued with TIRF microscopy (27).

Propofol Shortens the Run Length Potential of Kinesin-1 K560 in a Concentration-Dependent Manner but Does Not Alter the Velocity of Movement. In the absence of propofol, single-molecule experiments show that K560 steps along the MT at a rate of 309.3 nm/s with a run length of 1.03 μm (Fig. 2). Note that, in the presence of 3–5% DMSO, the concentration used as the propofol vehicle, the motility properties of K560, KIF3AC, or KIF3AB were not noticeably altered (Table S1). In contrast, the run length decreased to 0.58 μm in 10 μM propofol, but the velocity was similar at 282 nm/s (Fig. 2 *A* and *B* and Movies S3 and S4). This run length change is significant, because for processive kinesins, each 8-nm step is coupled to one ATP turnover. Thereby, propofol decreased kinesin processivity from ∼129 to 72 steps per run. Subsequent experiments evaluated a propofol concentration dependence, with each data point in Fig. 2 *C* and *D* representing the average run length and velocity from the Gaussian fit to each histogram dataset as shown for 10 μM propofol in Fig. 1 *A* and *B*. Fig. 2*C* shows that the average run length decreased as a function of propofol concentration, with the decrease becoming statistically significant at 5 nM propofol ($P < 0.002$), but the velocity at each propofol concentration was unaffected. Furthermore, the Hill–Slope model fit to the data provided the EC_{50} at 58.6 nM.

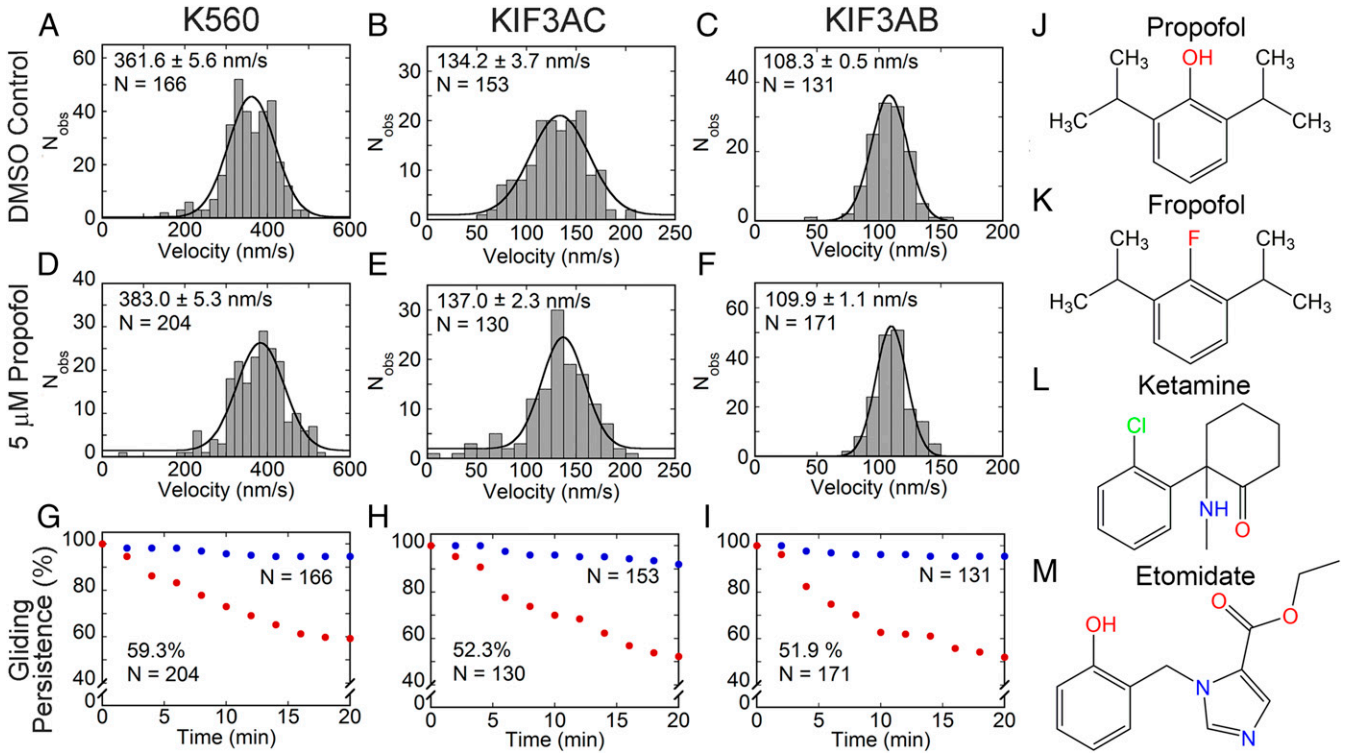

Fig. 1. Propofol disrupts the persistence of MT gliding but does not significantly alter the velocity of MT gliding. (*A*–*F*) Histograms of velocities (*A*–*C*) in control conditions (3% DMSO) and (*D*–*F*) at 5 μM propofol for each population of motors. A Gaussian fit provides the average velocity ±SEM for each dataset. The average velocities were not statistically significant between DMSO controls and 5 μM propofol datasets ($P > 0.5$). All experiments were conducted in the presence of 1 mM MgATP. Representative Movies S1 and S2 show K560. (*G*–*I*) Persistence of MT gliding as a function of time in 3% DMSO (blue) or 5 μM propofol (red). For all panels, *N* represents the number of MTs analyzed for each condition. (*A*, *D*, and *G*) Kinesin-1 K560, (*B*, *E*, and *H*) kinesin-2 KIF3AC, and (*C*, *F*, and *I*) kinesin-2 KIF3AB. (*J*–*M*) Anesthetics used in this report: (*J*) propofol, 2,6-diisopropylphenol; (*K*) fropofol, 2-fluoro-1,3-diisopropylbenzene; (*L*) ketamine, 2-(2-chlorophenyl)-2-(methylamino)cyclohexanone; and (*M*) etomidate, 1-(α-methylbenzyl)imidazole-5-carboxylic acid ethyl ester.

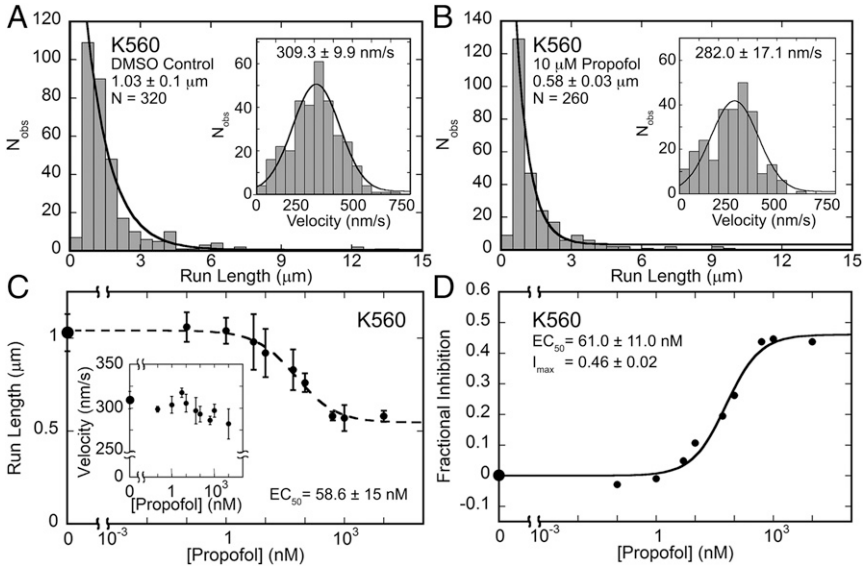

Fig. 2. Propofol shortens the mean run length of kinesin-1 K560 but does not alter velocity. (*A* and *B*) K560 run length and (*Insets*) velocity data in (*A*) 5% DMSO control and (*B*) 10 μM propofol. Statistical comparison of these data shows that the impact on run length is highly significant ($P < 0.0001$) but that the effect on velocity is not significant ($P > 0.9$). All experiments were conducted in the presence of 1 mM MgATP (Movies S3 and S4). (*C*) Mean run length and (*Inset*) velocity from K560 single-molecule motility assays plotted as a function of increasing propofol concentration over a range of 0 (5% DMSO control) to 10^6 nM propofol (log scale). The decrease in run length becomes statistically significant at 5 nM propofol ($P < 0.002$), whereas the variation in velocity is not statistically significant ($P > 0.5$). The EC_{50} was determined from fitting run length data to the Hill–Slope model. (*D*) Fractional inhibition of the run length data at each propofol concentration was plotted as a concentration dependence. The quadratic function provided the EC_{50} and the maximal fractional inhibition (I_{max}). All values are ±SEM.

To determine the maximal fractional inhibition, the data were analyzed as follows:

$$I = \frac{\text{Control RL} - \text{Propofol RL}}{\text{Control RL}},$$

where fractional inhibition, I, is defined as the difference between the run lengths (RL) of the DMSO control and each propofol concentration divided by the control run length (Fig. 2*D*). The following quadratic equation was fit to the data:

$$I = \frac{(I_{max} + P + EC_{50}) - \sqrt{(I_{max} + P + EC_{50})^2 - (4I_{max} \cdot P)}}{2},$$

where I_{max} is the maximal fractional inhibition, and P is the propofol concentration. The EC_{50} from this fit at 61 nM is comparable with the Hill–Slope model estimation at 58.6 nM. The maximal fractional inhibition at 0.46 revealed a significant decrease in K560 run length potential.

Propofol Also Shortens the Run Length Potential of Kinesin-2 KIF3AC and KIF3AB. Fig. 3 *A–D* shows the results for the KIF3AC single-molecule studies (Movies S5 and S6). Note that, in the presence of 10 μM propofol, the run length decreased significantly from 1.16 to 0.7 μm ($P < 0.0001$), but the velocities were unaffected. Like K560, the KIF3AC single-molecule experiments were repeated as a function of propofol concentration (Fig. 3*C*). The difference in run length became statistically significant at 0.25 nM propofol ($P < 0.0001$), whereas the velocity remained unchanged. The Hill–Slope model fit to the run length data provided an EC_{50} at 1.3 nM. Fig. 3*D* shows the data presented as the fractional inhibition at each propofol concentration. The quadratic fit to these data provided an EC_{50} at 0.93 nM and the maximal fractional inhibition of 0.40, indicating that propofol shortened the run length potential significantly. Moreover, the EC_{50} value at ~1 nM is very close to the concentration of the KIF3AC heterodimers in the perfusion chamber at 2 nM Qdot-bound KIF3AC, suggesting the possibility that KIF3A or KIF3C binds propofol more tightly than its partner motor head.

The impact of propofol on KIF3AB was also evaluated (Fig. 3 *E* and *F* and Movies S7 and S8). The results show that the 0.65-μm run length at 10 μM propofol was significantly less ($P < 0.0001$) than the run length in the absence of propofol at 1.61 μm. A propofol concentration dependence for KIF3AB was not pursued to determine the EC_{50}, but the 10 μM results clearly show that, as with K560 and KIF3AC, propofol also decreases the run length of KIF3AB considerably ($I_{max} = 0.60$) without impacting velocity ($P > 0.2$).

These results illustrate the remarkable impact that propofol has on the performance of these processive kinesins with EC_{50} values in the nanomolar range (Fig. 3*G*). Furthermore, the 40–60% decrease in run length potential suggests a common mechanism, especially based on the overall sequence homology between the catalytic core of the processive kinesin motor domains. Equally intriguing is that each of these processive kinesins could sustain sequential stepping at very high concentrations of propofol and maintain their normal velocity (Fig. 3*G*).

Propofol Inhibition Is Dependent on the Propofol Hydroxyl. Propofol is a fairly simple hydrophobic compound (Fig. 1*J*), but it contains the 1-hydroxyl that has been linked to molecular recognition within targets that contribute to anesthesia end points. Woll et al. (32) synthesized a compound named fropofol, in which the 1-hydroxyl was substituted with fluoride, dramatically reducing the ability to hydrogen bond (Fig. 1*K*). This analog maintains a similar molecular volume as propofol with a small increase in hydrophobicity, and fropofol also binds some of the molecular targets of propofol, such as apoferritin (32). With the 1-hydroxyl substitution, fropofol failed to induce loss of mobility end points in *Xenopus laevis* tadpoles and mice and does not enhance $GABA_A$ receptor activity. However, fropofol does retain the propofol-like ability to depress myocardial contractility (8, 32). Therefore, fropofol can be used to separate the desired from some undesired end points of anesthesia. To test the hypothesis that the 1-hydroxyl was necessary for the propofol effect on processive kinesins and thereby, potentially

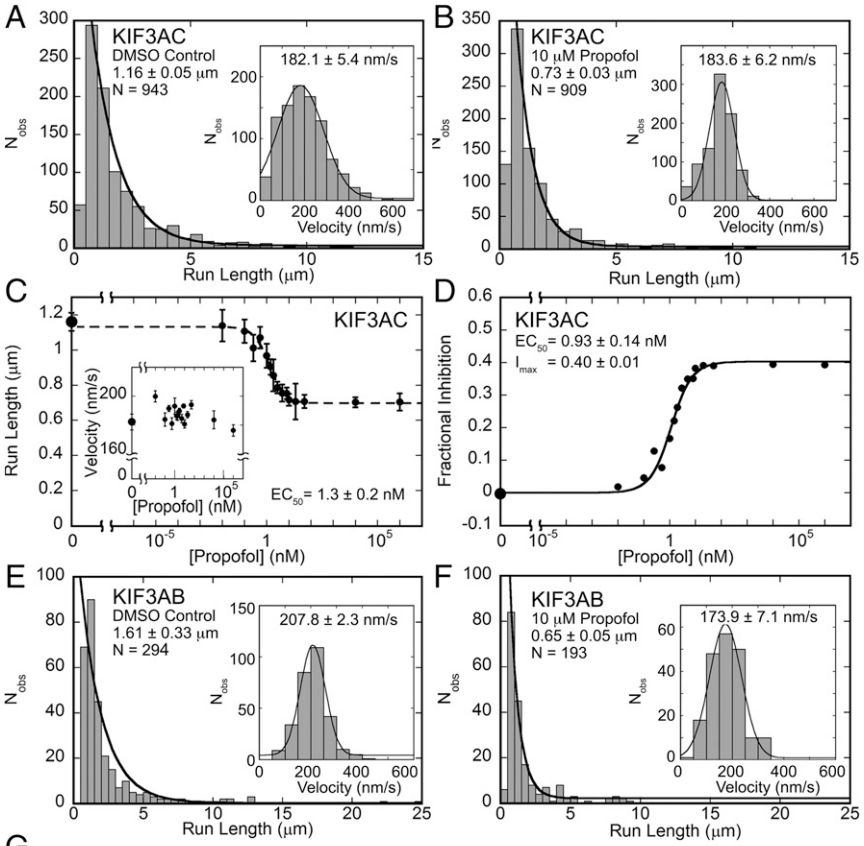

G

	DMSO		10 μM Propofol			
	Run Length (μm)	Velocity (nm/s)	Run Length (μm)	Velocity (nm/s)	I_{max}	EC_{50} (nM)
K560	1.03 ± 0.10	309.2 ± 9.9	0.58 ± 0.03	282.0 ± 17.0	0.46 ± 0.02	61.0 ± 11.0
KIF3AC	1.16 ± 0.05	182.1 ± 5.4	0.70 ± 0.03	183.6 ± 6.2	0.40 ± 0.01	0.93 ± 0.14
KIF3AB	1.61 ± 0.33	207.8 ± 2.3	0.65 ± 0.05	173.9 ± 7.1	0.60 ± 0.03*	—

Fig. 3. Propofol affects K560, KIF3AC, and KIF3AB motility similarly. (*A* and *B*) KIF3AC run length and (*Insets*) velocity data in (*A*) 5% DMSO control vs. (*B*) 10 μM propofol (Movies S5 and S6). (*C*) Average run length and (*Inset*) velocity data from KIF3AC single-molecule motility assays plotted as a function of increasing concentration from 0 (5% DMSO control) to 10^6 nM propofol (log scale). The difference in run length becomes statistically significant at 0.25 nM propofol ($P < <0.0001$), whereas there is no statistical significance between average velocities ($P > 0.4$). Run length data were fit to the Hill–Slope model, which provided the EC_{50}. (*D*) Fractional inhibition of the KIF3AC run length data at each propofol concentration was plotted as a concentration dependence. The quadratic function fit to the data provided an EC_{50} and the maximal fractional inhibition I_{max}. (*E* and *F*) KIF3AB run length and (*Insets*) velocity data in (*E*) 5% DMSO control vs. (*F*) 10 μM propofol (Movies S7 and S8). The decrease in run length is highly statistically significant ($P < <0.0001$), whereas velocity does not exhibit a statistical difference in the presence of propofol ($P > 0.2$). (*G*) Compiled single-molecule motility data from Fig. 2 and this figure. All experiments were conducted in the presence of 1 mM MgATP, and all values are ±SEM. *I_{max} for KIF3AB is calculated based on the fractional inhibition at 10 μM propofol (*E* and *F*).

attribute this effect to desired end points of anesthesia, we pursued single-molecule experiments with KIF3AC at 10 and 100 μM fropofol. Fig. 4 shows that, even at 100 μM fropofol, neither the run length of KIF3AC ($P > 0.6$) nor the KIF3AC velocity ($P > 0.3$) were significantly diminished. These results clearly show that the propofol 1-hydroxyl is critical for molecular recognition and/or

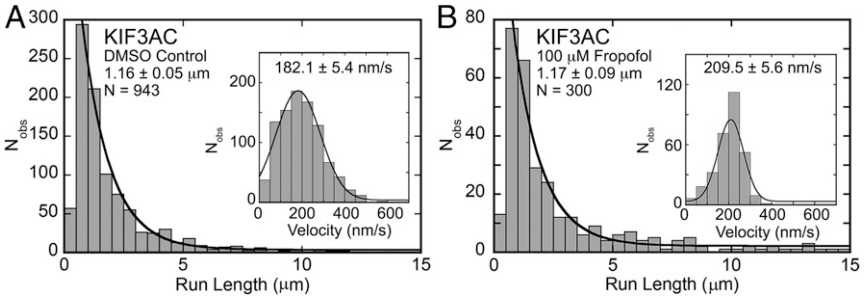

Fig. 4. Fropofol does not inhibit KIF3AC run length or velocity. KIF3AC run length and (*Insets*) velocity data in the presence of (*A*) 5% DMSO control and (*B*) 100 μM fropofol. Neither the difference in run length nor the velocity were statistically significant ($P > 0.3$). All values are reported as the average from the fit of the histogram ±SEM.

kinesin run length inhibition and that kinesins may contribute to propofol-induced unconsciousness as reflected by loss of mobility end points.

Propofol Shortens the Run Length Potential of Homodimeric KIF3BB and KIF3CC, but No Effect Is Observed for KIF3AA. We were intrigued by the EC_{50} at ~1 nM propofol for KIF3AC, because the single-molecule experiments were performed at 2 nM KIF3AC dimer. We questioned whether this constant may reflect a difference in propofol binding affinity to KIF3A compared with KIF3C. To explore this hypothesis further, single-molecule experiments at 10 μM propofol were pursued with engineered homodimers of KIF3AA, KIF3BB, and KIF3CC (Fig. 5). The homodimer design was similar to that of the heterodimers, where each polypeptide included the native catalytic motor domain, the neck linker, helix α7 followed by a dimerization domain, the Tobacco Etch Virus site, and the His_8 tag (27). The results were surprising. Although 10 μM propofol shortened the run length potentials of homodimeric KIF3BB ($I_{max} = 0.56$) and KIF3CC ($I_{max} = 0.38$), propofol seemed to have negligible effect on KIF3AA ($I_{max} = 0.02$).

When the sequences of the motor domain were compared, KIF3B and KIF3C show 71% identity, but the identity between KIF3A and KIF3B or KIF3C is less at 69 and 57%, respectively. Kinesin-1 KIF5B was clearly affected by propofol, but its sequence identity compared with KIF3A, KIF3B, and KIF3C is less than 50%. However, structurally kinesins share a highly conserved Walker nucleotide binding fold that consists of a central twisted β-sheet and three nucleotide binding loops designated switch-1, switch-2, and the P loop (33–37). Kinesins also share a similar MT binding interface and a series of structural transitions in response to the nucleotide binding state that coordinates MT association and detachment (38–41). To sustain a processive run, the domains must be coordinated, so that one is always in a MT strongly bound state to prevent motor detachment from the MT (42–44). Therefore, these results suggest that, despite the relatively high homology between these motor domains, small sequence differences in the motor domain have resulted in KIF3A either not binding propofol and/or propofol not promoting premature motor detachment from the MT.

Etomidate and Ketamine Also Inhibit the Run Length Potential of KIF3AC. General anesthetics have multiple functional targets and overlapping binding sites within their target proteins, in part because they are small hydrophobic molecules. To determine if processive kinesins are affected by other i.v. general anesthetics, we tested whether kinesin motility of KIF3AC was altered by ketamine or etomidate (Fig. 1 *L* and *M*). Etomidate, like propofol, enhances the $GABA_A$-mediated inhibitory response, whereas ketamine acts primarily as an antagonist of NMDA receptors, although it too has multiple targets, including a subset of the G protein (heterotrimeric

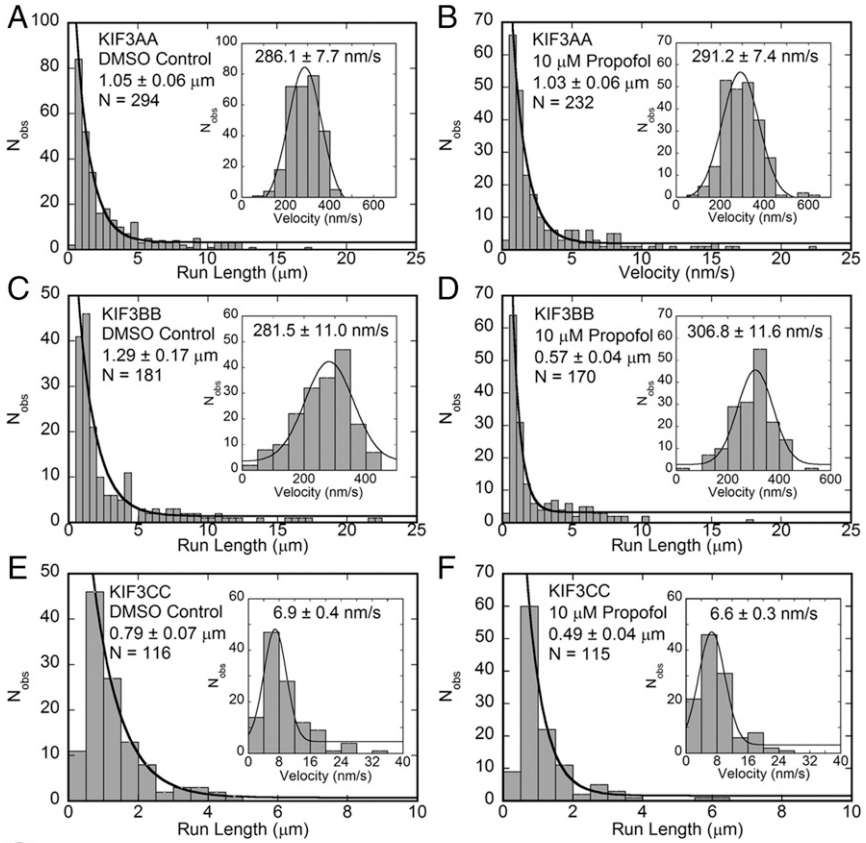

G

	DMSO		10 μM Propofol		
	Run Length (μm)	Velocity (nm/s)	Run Length (μm)	Velocity (nm/s)	I_{max}
KIF3AA	1.05 ± 0.06	286.1 ± 7.7	1.03 ± 0.06	291.2 ± 7.4	0.02
KIF3BB	1.29 ± 0.17	281.5 ± 11.0	0.57 ± 0.04	306.8 ± 11.8	0.56
KIF3CC	0.79 ± 0.07	6.9 ± 0.04	0.49 ± 0.04	6.6 ± 0.03	0.38

Fig. 5. Propofol does not affect homodimeric KIF3AA single-molecule motility. (*A*–*F*) Single-molecule run length and (*Insets*) velocity data for (*A* and *B*) KIF3AA, (*C* and *D*) KIF3BB, and (*E* and *F*) KIF3CC comparing control conditions at (*A*, *C*, and *E*) 5% DMSO vs. (*B*, *D*, and *F*) 10 μM propofol. All experiments were conducted at 1 mM MgATP. (*G*) Compiled single-molecule motility data. I_{max} is calculated based on the fractional inhibition at 10 μM propofol.

guanine nucleotide binding protein)-coupled receptors that are distributed throughout the CNS (10–14). The results in Fig. S1 show that, like propofol, 10 μM etomidate or ketamine shortened the run length potential of kinesin-2 KIF3AC: from 1.19 to 0.57 μm by etomidate and from 1.19 to 0.52 μm by ketamine ($P < 0.0001$). Also, like propofol, neither drug altered the velocity of movement significantly ($P > 0.7$). These results implicate processive kinesins as anesthetic targets that may contribute to modulation of the anesthetic state.

Discussion

There Is a Common Mechanism to Shorten Run Length Potential. Because propofol did not alter the velocity of movement for K560, KIF3AC, or KIF3AB in the MT gliding or single-molecule experiments, we propose that propofol is not binding at allosteric sites within the catalytic motor domain that would alter MT-activated ATP turnover. Moreover, because the concentration of MTs is at 0.1 μM in the single-molecule assays and the EC_{50} values are <100 nM propofol, it is unlikely that propofol is saturating binding sites along the MT where the kinesin head would step during a processive run. Moreover, the lack of a propofol effect on KIF3AA renders a common MT site unlikely. Rather, these results indicate that propofol and likely, etomidate and ketamine allosteric binding sites form transiently in kinesin when the motor domain binds to the MT lattice during stepping, reducing kinesin MT affinity. This outcome, in essence, implies a druggable allosteric site that, when occupied, promotes detachment of the kinesin motor from the MT. There may exist multiple transient propofol and therefore, etomidate and ketamine binding sites on the kinesin motor domain, requiring only anesthetic binding to kinesin to impact the motor's interactions with the MT. Note too that the maximal fractional inhibition promoted by propofol, etomidate, and ketamine was 0.4–0.6, suggesting a common mechanism for shortening the run length of these kinesins. This inhibition profile is very different from the loop L5-targeting small-molecule drugs in either the monastrol family of inhibitors for human kinesin-5 KSP/Eg5 (45–48) or the kinesin-specific inhibitor GSK923295 for kinesin-7 CENP-E (49). Monastrol family inhibitors stabilize ADP at the active site and therefore, destabilize the MT–KSP interaction. GSK923295 inhibits the release of inorganic phosphate and stabilizes the interaction of CENP-E with the MT. However, both inhibitors alter MT-activated ATPase activity as well as kinesin-promoted motility, which is very different from the results presented here.

One can reason based on kinesin X-ray crystal structures and site-specific mutations that small, hydrophobic anesthetic molecules have the potential to bind at multiple allosteric sites on the kinesin motor domain or at residues of the MT•kinesin interface to alter kinesin binding affinity to the MT and promote motor detachment (38, 39, 50–54).

Are Processive Kinesins Targets of General Anesthetics, and Thereby, Do They Contribute to the Anesthetic State? The binding of general anesthetics to ligand- or voltage-gated channels and receptors is known to elicit both desired and undesired end points of anesthesia. However, it is also recognized that none of these molecular targets have satisfied the criteria of being both necessary and sufficient to produce the complete anesthetic state. Other plausible targets have included mitochondria, tubulin, and the synaptic vesicle transport and release machinery (17, 55–58). For example, SNAP-25 and syntaxin specifically bind propofol (7). Therefore, it is reasonable that there are other targets that interact with anesthetics and contribute to the state of anesthesia. Our results expand the field by providing evidence for a largely overlooked but critically positioned set of targets, molecular motors, which could influence acute and/or chronic end points observed with some general anesthetics.

The EC_{50} values for kinesin "derailing" are at least 10-fold lower than those associated with propofol-induced immobility, suggesting that these effects may underlie other subclinical actions of propofol, such as amnesia and postural instability. Alternatively, it is possible that EC_{50} values will be very different in the crowded intracellular milieu and when the motors are loaded with cargo. Nevertheless, these results clearly indicate that kinesin motors will be influenced during propofol anesthesia in vivo, and it seems unlikely that such important intracellular movers will not contribute to components of anesthetic action.

The human kinesin superfamily includes 45 genes, 38 of which are expressed in brain, with three subfamilies of kinesins that are predominantly responsible for cargo transport to the cell periphery (i.e., the synapse in neurons) (21, 22, 24, 25, 30, 59, 60). Kinesins are the major anterograde transporters of cargos that have been established as anesthetic targets, including mitochondria, $GABA_A$ receptors, syntaxin, and SNAP-25 (7, 9, 57, 58, 61–64). The critical neurological role of kinesins is further indicated by the lethality of many mutations, an anesthetic-like immobility phenotype in others, and numerous kinesin dysfunctions linked to a wide range of human pathologies, including neurodevelopmental and neurodegenerative diseases, ciliopathies, epilepsy, and birth defects (21, 24, 64–67).

In summary, the flux of cellular substrates is a balance between the collective anterograde transport by kinesins and retrograde transport by dynein. Even a modest depletion of kinesin-1 or -2 processivity would create an opportunity for retrograde motors, like dynein, to drive cargo transport back to the cell body, leading to a critical imbalance of cargo distribution. Therefore, kinesins are critically positioned to underlie specific anesthesia end points, and this report has revealed a dramatic impact of three different anesthetics on processive kinesins at concentrations used in routine clinical care.

Methods

Standard MT gliding and single-molecule kinesin Qdot assays and TIRF imaging techniques were used throughout. Detailed descriptions of kinesin motor construct design, expression, and purification and microscopy methods are provided in *SI Methods*. MT concentrations are reported as paclitaxel-stabilized α,β-tubulin concentration.

ACKNOWLEDGMENTS. We thank Pei Tang (Department of Anesthesiology, University of Pittsburgh) for her initial suggestion that propofol might affect kinesin motility and Nicole Stoddard, who initiated this project as her Rensselaer Senior Research Thesis. This work was supported, in part, by an award from the Rensselaer Office of Research, National Science Foundation Graduate Research Fellowship Program Grant DGE-1321851 (to K.A.W.), and NIH Grants P01-GM55876 (to R.G.E.) and R37-GM054141 (to S.P.G.).

1. Kotani Y, Shimazawa M, Yoshimura S, Iwama T, Hara H (2008) The experimental and clinical pharmacology of propofol, an anesthetic agent with neuroprotective properties. *CNS Neurosci Ther* 14:95–106.
2. Bateman BT, Kesselheim AS (2015) Propofol as a transformative drug in anesthesia: Insights from key early investigators. *Drug Discov Today* 20:1012–1017.
3. Krasowski MD, et al. (2001) General anesthetic potencies of a series of propofol analogs correlate with potency for potentiation of gamma-aminobutyric acid (GABA) current at the GABA(A) receptor but not with lipid solubility. *J Pharmacol Exp Ther* 297:338–351.
4. Stewart DS, et al. (2011) p-(4-Azipentyl)propofol: A potent photoreactive general anesthetic derivative of propofol. *J Med Chem* 54:8124–8135.
5. Chiara DC, et al. (2014) Photoaffinity labeling the propofol binding site in GLIC. *Biochemistry* 53:135–142.
6. Jayakar SS, et al. (2014) Multiple propofol-binding sites in a γ-aminobutyric acid type A receptor (GABAAR) identified using a photoreactive propofol analog. *J Biol Chem* 289:27456–27468.
7. Woll KA, et al. (2016) A novel bifunctional alkylphenol anesthetic allows characterization of γ-aminobutyric acid, type A (GABAA), receptor subunit binding selectivity in synaptosomes. *J Biol Chem* 291:20473–20486.
8. Meng T, et al. (2016) Molecular mechanism of anesthetic-induced depression of myocardial contraction. *FASEB J* 30:2915–2925.
9. Woll KA, Dailey WP, Brannigan G, Eckenhoff RG (2016) Shedding light on anesthetic mechanisms: Application of photoaffinity ligands. *Anesth Analg* 123:1253–1262.
10. Rudolph U, Antkowiak B (2004) Molecular and neuronal substrates for general anaesthetics. *Nat Rev Neurosci* 5:709–720.

11. Brown EN, Purdon PL, Van Dort CJ (2011) General anesthesia and altered states of arousal: A systems neuroscience analysis. *Annu Rev Neurosci* 34:601–628.
12. Erdoes G, Basciani RM, Eberle B (2014) Etomidate–a review of robust evidence for its use in various clinical scenarios. *Acta Anaesthesiol Scand* 58:380–389.
13. Ho J, et al. (2015) Molecular recognition of ketamine by a subset of olfactory G protein-coupled receptors. *Sci Signal* 8:ra33.
14. Li L, Vlisides PE (2016) Ketamine: 50 Years of modulating the mind. *Front Hum Neurosci* 10:612.
15. Kaech S, Brinkhaus H, Matus A (1999) Volatile anesthetics block actin-based motility in dendritic spines. *Proc Natl Acad Sci USA* 96:10433–10437.
16. Turina D, Bjornstrom K, Sundqvist T, Eintrei C (2011) Propofol alters vesicular transport in rat cortical neuronal cultures. *J Physiol Pharmacol* 62:119–124.
17. Emerson DJ, et al. (2013) Direct modulation of microtubule stability contributes to anthracene general anesthesia. *J Am Chem Soc* 135:5389–5398.
18. Craddock TJ, et al. (2012) Computational predictions of volatile anesthetic interactions with the microtubule cytoskeleton: Implications for side effects of general anesthesia. *PLoS One* 7:e37251.
19. Craddock TJ, Priel A, Tuszynski JA (2014) Keeping time: Could quantum beating in microtubules be the basis for the neural synchrony related to consciousness? *J Integr Neurosci* 13:293–311.
20. Miki H, Setou M, Kaneshiro K, Hirokawa N (2001) All kinesin superfamily protein, KIF, genes in mouse and human. *Proc Natl Acad Sci USA* 98:7004–7011.
21. Hirokawa N, Niwa S, Tanaka Y (2010) Molecular motors in neurons: Transport mechanisms and roles in brain function, development, and disease. *Neuron* 68:610–638.
22. Verhey KJ, Kaul N, Soppina V (2011) Kinesin assembly and movement in cells. *Annu Rev Biophys* 40:267–288.
23. Scholey JM (2013) Kinesin-2: A family of heterotrimeric and homodimeric motors with diverse intracellular transport functions. *Annu Rev Cell Dev Biol* 29:443–469.
24. Maday S, Twelvetrees AE, Moughamian AJ, Holzbaur EL (2014) Axonal transport: Cargo-specific mechanisms of motility and regulation. *Neuron* 84:292–309.
25. Bentley M, Banker G (2016) The cellular mechanisms that maintain neuronal polarity. *Nat Rev Neurosci* 17:611–622.
26. Sardar HS, Luczak VG, Lopez MM, Lister BC, Gilbert SP (2010) Mitotic kinesin CENP-E promotes microtubule plus-end elongation. *Curr Biol* 20:1648–1653.
27. Guzik-Lendrum S, et al. (2015) Kinesin-2 KIF3AC and KIF3AB can drive long-range transport along microtubules. *Biophys J* 109:1472–1482.
28. Tomishige M, Vale RD (2000) Controlling kinesin by reversible disulfide cross-linking. Identifying the motility-producing conformational change. *J Cell Biol* 151:1081–1092.
29. Yildiz A, Tomishige M, Gennerich A, Vale RD (2008) Intramolecular strain coordinates kinesin stepping behavior along microtubules. *Cell* 134:1030–1041.
30. Hirokawa N, Noda Y, Tanaka Y, Niwa S (2009) Kinesin superfamily motor proteins and intracellular transport. *Nat Rev Mol Cell Biol* 10:682–696.
31. Albracht CD, Rank KC, Obrzut S, Rayment I, Gilbert SP (2014) Kinesin-2 KIF3AB exhibits novel ATPase characteristics. *J Biol Chem* 289:27836–27848.
32. Woll KA, et al. (2015) Role for the propofol hydroxyl in anesthetic protein target molecular recognition. *ACS Chem Neurosci* 6:927–935.
33. Kull FJ, Sablin EP, Lau R, Fletterick RJ, Vale RD (1996) Crystal structure of the kinesin motor domain reveals a structural similarity to myosin. *Nature* 380:550–555.
34. Gigant B, et al. (2013) Structure of a kinesin-tubulin complex and implications for kinesin motility. *Nat Struct Mol Biol* 20:1001–1007.
35. Cao L, et al. (2014) The structure of apo-kinesin bound to tubulin links the nucleotide cycle to movement. *Nat Commun* 5:5364.
36. Shang Z, et al. (2014) High-resolution structures of kinesin on microtubules provide a basis for nucleotide-gated force-generation. *eLife* 3:e04686.
37. Morikawa M, et al. (2015) X-ray and Cryo-EM structures reveal mutual conformational changes of Kinesin and GTP-state microtubules upon binding. *EMBO J* 34:1270–1286.
38. Woehlke G, et al. (1997) Microtubule interaction site of the kinesin motor. *Cell* 90: 207–216.
39. Klumpp LM, et al. (2004) Microtubule-kinesin interface mutants reveal a site critical for communication. *Biochemistry* 43:2792–2803.
40. Klumpp LM, Hoenger A, Gilbert SP (2004) Kinesin's second step. *Proc Natl Acad Sci USA* 101:3444–3449.
41. Rice S, et al. (1999) A structural change in the kinesin motor protein that drives motility. *Nature* 402:778–784.
42. Asbury CL, Fehr AN, Block SM (2003) Kinesin moves by an asymmetric hand-over-hand mechanism. *Science* 302:2130–2134.
43. Kaseda K, Higuchi H, Hirose K (2003) Alternate fast and slow stepping of a heterodimeric kinesin molecule. *Nat Cell Biol* 5:1079–1082.
44. Yildiz A, Tomishige M, Vale RD, Selvin PR (2004) Kinesin walks hand-over-hand. *Science* 303:676–678.
45. Mayer TU, et al. (1999) Small molecule inhibitor of mitotic spindle bipolarity identified in a phenotype-based screen. *Science* 286:971–974.
46. Kapoor TM, Mayer TU, Coughlin ML, Mitchison TJ (2000) Probing spindle assembly mechanisms with monastrol, a small molecule inhibitor of the mitotic kinesin, Eg5. *J Cell Biol* 150:975–988.
47. Yan Y, et al. (2004) Inhibition of a mitotic motor protein: Where, how, and conformational consequences. *J Mol Biol* 335:547–554.
48. Ulaganathan V, et al. (2013) Structural insights into a unique inhibitor binding pocket in kinesin spindle protein. *J Am Chem Soc* 135:2263–2272.
49. Wood KW, et al. (2010) Antitumor activity of an allosteric inhibitor of centromere-associated protein-E. *Proc Natl Acad Sci USA* 107:5839–5844.
50. Klumpp LM, Brendza KM, Rosenberg JM, Hoenger A, Gilbert SP (2003) Motor domain mutation traps kinesin as a microtubule rigor complex. *Biochemistry* 42:2595–2606.
51. Tischfield MA, et al. (2010) Human TUBB3 mutations perturb microtubule dynamics, kinesin interactions, and axon guidance. *Cell* 140:74–87.
52. Djagaeva I, et al. (2012) Three routes to suppression of the neurodegenerative phenotypes caused by kinesin heavy chain mutations. *Genetics* 192:173–183.
53. Niwa S, Takahashi H, Hirokawa N (2013) β-Tubulin mutations that cause severe neuropathies disrupt axonal transport. *EMBO J* 32:1352–1364.
54. Minoura I, et al. (2016) Reversal of axonal growth defects in an extraocular fibrosis model by engineering the kinesin-microtubule interface. *Nat Commun* 7:10058.
55. Falk MJ, Kayser EB, Morgan PG, Sedensky MM (2006) Mitochondrial complex I function modulates volatile anesthetic sensitivity in C. elegans. *Curr Biol* 16:1641–1645.
56. Chen ZW, et al. (2012) A neurosteroid analogue photolabeling reagent labels the colchicine-binding site on tubulin: A mass spectrometric analysis. *Electrophoresis* 33:666–674.
57. Zalucki OH, et al. (2015) Syntaxin1A-mediated resistance and hypersensitivity to isoflurane in Drosophila melanogaster. *Anesthesiology* 122:1060–1074.
58. MacDonald JI, et al. (2012) Nesca, a novel neuronal adapter protein, links the molecular motor kinesin with the pre-synaptic membrane protein, syntaxin-1, in hippocampal neurons. *J Neurochem* 121:861–880.
59. Huang CF, Banker G (2012) The translocation selectivity of the kinesins that mediate neuronal organelle transport. *Traffic* 13:549–564.
60. Liu XA, et al. (2014) New approach to capture and characterize synaptic proteome. *Proc Natl Acad Sci USA* 111:16154–16159.
61. van Swinderen B, et al. (1999) A neomorphic syntaxin mutation blocks volatile-anesthetic action in Caenorhabditis elegans. *Proc Natl Acad Sci USA* 96:2479–2484.
62. Nagele P, et al. (2005) Volatile anesthetics bind rat synaptic snare proteins. *Anesthesiology* 103:768–778.
63. Cai Q, Pan PY, Sheng ZH (2007) Syntabulin-kinesin-1 family member 5B-mediated axonal transport contributes to activity-dependent presynaptic assembly. *J Neurosci* 27:7284–7296.
64. Nakajima K, et al. (2012) Molecular motor KIF5A is essential for GABA(A) receptor transport, and KIF5A deletion causes epilepsy. *Neuron* 76:945–961.
65. Tanaka Y, et al. (1998) Targeted disruption of mouse conventional kinesin heavy chain, kif5B, results in abnormal perinuclear clustering of mitochondria. *Cell* 93:1147–1158.
66. Marszalek JR, Ruiz-Lozano P, Roberts E, Chien KR, Goldstein LS (1999) Situs inversus and embryonic ciliary morphogenesis defects in mouse mutants lacking the KIF3A subunit of kinesin-II. *Proc Natl Acad Sci USA* 96:5043–5048.
67. Hirokawa N, Tanaka Y (2015) Kinesin superfamily proteins (KIFs): Various functions and their relevance for important phenomena in life and diseases. *Exp Cell Res* 334:16–25.
68. Lindhout DA, Litowski JR, Mercier P, Hodges RS, Sykes BD (2004) NMR solution structure of a highly stable de novo heterodimeric coiled-coil. *Biopolymers* 75:367–375.
69. Rank KC, et al. (2012) Kar3Vik1, a member of the kinesin-14 superfamily, shows a novel kinesin microtubule binding pattern. *J Cell Biol* 197:957–970.
70. Bu W, Su LK (2003) Characterization of functional domains of human EB1 family proteins. *J Biol Chem* 278:49721–49731.
71. Komaki S, et al. (2010) Nuclear-localized subtype of end-binding 1 protein regulates spindle organization in Arabidopsis. *J Cell Sci* 123:451–459.